Polymer 51 (2010) 4978–4984

Contents lists available at ScienceDirect

Polymer

journal homepage: www.elsevier.com/locate/polymer

Molecular simulations of the solubility of gases in polyethylene below its melting temperature

Peyman Memari [a,b], Véronique Lachet [b], Bernard Rousseau [a,*]

[a] Laboratoire de Chimie Physique, Université Paris Sud, UMR 8000 CNRS, 91405 Orsay Cedex, France
[b] IFP Energies nouvelles, 1 & 4 avenue de Bois-Préau, 92852 Rueil-Malmaison Cedex, France

ARTICLE INFO

Article history:
Received 13 April 2010
Received in revised form
5 August 2010
Accepted 9 August 2010
Available online 17 August 2010

Keywords:
Polymer
Physical
Chemistry

ABSTRACT

We have employed Monte Carlo simulations in the osmotic ensemble to study the solubility of three different gases (N_2, CH_4, CO_2) in polyethylene. The simulations are performed at temperatures below the polymer melting point. Although under such conditions, polyethylene is in a semicrystalline state, we have used simulation boxes containing only a purely amorphous material. We show that under such circumstances, computed solubilities are 4–5 times larger than experimental data. We therefore introduce an original use of the osmotic ensemble to implicitly account for the effects of the complex morphology of semicrystalline materials on gas solubility. We have made the assumption that i) the network formed by polymer chains trapped between different crystallites and ii) the changes in local density from crystalline regions to purely amorphous regions, may be both represented by an *ad-hoc* constraint exerted on the amorphous phase. A single constraint value emerges, independent of the gas nature, characteristic of the crystalline degree of the polymer. It is concluded that the role of this constraint is mostly to reproduce the effective density of the permeable phase of the real material, indirectly giving insights into the morphology of a semicrystalline polymer.

1. Introduction

Polymers are used in many industrial applications as barriers to protect materials from gas or liquid contamination. The relevant quantity involved in this process is the permeability, *P*, which quantifies the amount of matter passing through the polymer phase per unit time and unit area. Permeability is the product of two terms: the solubility, *S*, describing the solute concentration into the polymer phase and the diffusion coefficient, *D*, describing the solute mass transport inside the polymer. Therefore, a complete description and understanding of permeability requires the knowledge of both solubility and mass diffusion of permeant into the permeable phase.

Molecular simulation is an attractive tool to calculate such properties as it relies on methods with few assumptions and is based on well-defined molecular characteristics. Thanks to the increase of available computing power and to new methodological developments, several authors have investigated the modelling of gas permeability in polymers at a molecular level. Almost two decades ago, Suter and coll. [1] computed the solubility at infinite dilution of methane in frozen glassy polycarbonate. Müller-Plathe [2] used a test particle insertion method similar to Widom's method [3] to compute Henry's constant of different gases (helium, hydrogen, nitrogen, oxygen and methane) in models of amorphous atactic polypropylene. A few years later, de Pablo et al. [4] went beyond the computation of Henry's constant: using Gibbs ensemble Monte Carlo simulations and configurational bias moves, the solubility of short chain alkanes was computed in polyethylene melts, at gas pressures above Henry's regime. Amongst the pioneers in this area, Boyd and coll. [5] investigated the transport properties of small penetrants in amorphous polyethylene and polyisobutylene. In the following years, several studies have followed, considering many different penetrant gases and more complex polymers such as polypropylene [6], polystyrene [7], poly(styrene-*alt*-maleic anhydride) copolymer, poly (styrene-*stat*-butadiene) rubber [8], polyimides [9], polyethylene terephtalate and more [10].

In the present work, we would like to put emphasis on the computation of solubility of penetrant molecules into a *semicrystalline* polymer. Indeed, in most of the previous works presented above, solubility has been obtained either in melt or purely amorphous polymer, or, in the case of semicrystalline materials, within the assumptions that i) the amorphous phase is the only permeable phase and ii) the amorphous phase characteristics are not affected by the presence of the crystalline regions.

* Corresponding author. Laboratoire de Chimie Physique, Université Paris Sud, UMR 8000 CNRS, 91405 Orsay Cedex, France. Tel.: +331 6915 3030; fax: +331 6915 6188.
E-mail address: bernard.rousseau@u-psud.fr (B. Rousseau).

0032-3861/$ – see front matter © 2010 Elsevier Ltd. All rights reserved.
doi:10.1016/j.polymer.2010.08.020

The first hypothesis is strongly supported by experimental evidences. Experiments by Michaels and Bixler [11] on different polyethylene grades with different degrees of crystallinity permitted to establish the following relationship between the solubility in the semicrystalline material, S, *versus* the solubility in the amorphous phase, S_a:

$$S = S_a(1 - \chi), \tag{1}$$

where χ is the (volume or mass) fraction of the crystalline regions. Some recent work by Compañ et al. [12] suggests that the above rule is confirmed in the case of ethylene and propane in linear low density polyethylene although some slight deviations are observed. However, from a quantitative point of view, deviations from equation (1) remain negligible.

The second hypothesis clearly doesn't hold. In semicrystalline materials, the amorphous phase is perturbed by the presence of crystallites. These perturbations can be separated into two different contributions: an "elastic" effect and a "local density" effect.

The first contribution comes from the fact that some polymer chains leaving a crystalline region may be trapped in an other different crystalline region. The network formed by these tie segments has been considered as cross-links, restricting the swelling of polymer during the sorption process [13,14]. This effect, called the elastic effect, has been invoked by several authors to correct the predicted solubilities from the amorphous to the semicrystalline solubility. The correction term is usually introduced as a contribution term to the activity of the penetrant. A modified equation of state is therefore used that allows calculation of thermodynamics properties including the elastic effect contribution [13,15–17].

The local density effect is related to the interfacial complex morphology of semicrystalline materials. It was put forward during the late 40's by Flory [18], then working on lattice models: "The tacit assumption that the internal order changes abruptly from crystalline to complete randomness within one layer of lattice cells at the end of a crystallite is inherently fallacious. Such a sharp disappearance of order cannot occur in the lattice model, and this aspect of the model probably holds for the actual polymer as well. Some degree of order may persist for several layers beyond the end of a crystallite". In the following years, many experimental studies have demonstrated the presence of an appreciable interfacial region characterised by the partial ordering of chain segments (see e.g. the review paper by Mandelkern [19] and references therein). This continuous change from an ordered region to a disordered amorphous phase must be accompanied at least by a change in density and local chain mobility with important consequences on solubility and transport properties [20].

Indeed, several authors have reported large deviations between experimental data and theoretical predictions when they assume that the amorphous phase properties remain unaffected by the crystalline regions. Using Monte Carlo simulations, Nath and de Pablo [21] found that crystallinity can severely impact the solubility of small molecules in semicrystalline polyethylene, especially for highly soluble gases. Using the same molecular approach, Hu and Fried [22] also reported solubility coefficients of small gas molecules in poly (organophosphazenes) five times larger than what would be expected by extrapolating values reported for semicrystalline samples to 100% amorphous content.

Therefore, it would be relevant to undertake a molecular simulation with an explicit representation of a semicrystalline polymer. Unfortunately, the length scale involved in the description of such system is out of range of standard computers. Today's routinely accessible simulation box sizes for dense systems are of the order of 5 nm, below the typical dimension of a single crystallite. This led us to the development of an original methodology where crystalline regions are not explicitely described whereas their overall effect on the amorphous phase is accounted for. Our reasoning (hypothesis) is the following: elastic effects and changes in local density may be represented by an *ad-hoc* constraint exerted on the amorphous phase. This constraint must be characteristic of a material with a given crystallinity. We propose a method to obtain this constraint value so as to reproduce the solubility of experimentally well referenced systems. We will apply this methodology to polyethylene (PE), because of its wide use in industrial applications and its relative simplicity as a molecular model. The solubility of three different gases will be investigated: carbon dioxide, methane and nitrogen, mostly chosen because of their different solubilities in PE.

In the next section, we will present the methodological aspects of this work. In Section 3, we will rapidly review the experimental solubility data we have used in order to calibrate and validate our approach. In Section 4, we will present our simulation results on gas solubility and associated polymer swelling. A discussion on the magnitude of the proposed constraint value is also provided. Section 5 gives our conclusions.

2. Methodology

2.1. A specific use of the osmotic ensemble

The experimental situation we would like to describe is that of a polymer sample in equilibrium with a gas or a gas mixture at a given temperature T and pressure P. The polymer rich phase must be allowed to swell and the gas composition in the gas phase, $\{x_i\}$, must be constant during the permeation process. The so-called osmotic ensemble [23–26] is perfectly adapted to describe such an experimental situation. In this ensemble, a single phase (in our case, the polymer rich phase) is represented. This phase contains a fixed amount of polymer chains, N_p, in equilibrium with a gas or gas mixture with imposed chemical potential μ_i for each gas species i. Temperature and pressure are also imposed. This requires a preliminary simulation of the gas mixture at P, T and $\{x_i\}$ in order to obtain the chemical potential of each species in the gas phase under the "experimental conditions".

The osmotic ensemble presents several advantages over other statistical ensembles typically employed in the study of gas solubility in polymers. In the Henry's regime (low gas pressure), the solubility of a solute can be related to its excess free energy [2,4], a quantity that can be obtained in molecular simulations using the Widom insertion tests method [3]. Because no gas molecules are effectively inserted in the gas phase, deviations from the ideal behaviour cannot be observed. Simulations in the Grand Canonical ensemble are conducted at constant volume, hence, no swelling effect can be observed. Simulations in the Gibbs ensemble [27] can be performed at constant pressure so that non ideal effects and swelling can be studied. However, the gas phase composition is a result of a Gibbs ensemble simulation and therefore is not imposed. Moreover, it requires the simultaneous simulation of two boxes, the polymer rich phase and the gas phase, an unnecessary condition in the osmotic ensemble.

The osmotic ensemble has an other advantage in our case study. The pressure imposed to the polymer rich phase can be seen as an isotropic constraint σ_{iso}. In usual applications of the osmotic ensemble, the isotropic constraint value is set to the gas pressure. In this work, we will make an original use of the osmotic ensemble by distinguishing the gas pressure from the total constraint applied onto the polymer phase. The difference will correspond to the *ad-hoc* constraint σ that we want to apply to model implicitly the effect of crystallites onto the amorphous phase. As mentioned above, the gas pressure (along with its temperature and composition) will be controlled by the chemical potential of the different species as computed in a separate simulation.

In the osmotic ensemble, the number of polymer molecules N_p is kept constant whereas the number of molecules of the n gas species is variable. The configurational part of the partition function in this ensemble is given by the following expression:

$$\Theta = \sum_{V}\sum_{N_i}\sum_{U}\exp\left[-\beta U + \sum_{j=1}^{n}\beta\mu_j N_j - \beta\sigma_{\mathrm{iso}}V\right] \quad (2)$$

where $\beta = 1/k_BT$ with k_B the Boltzmann constant. N_i is the number of molecules of gas species i, V is the volume of the simulation box, μ_i is the chemical potential of the gas species i and U is the potential energy of the system. This expression is consistent with those found in previous works [25,26].

2.2. Monte Carlo moves

An efficient sampling of the configurational space of polymer chains requires the use of Monte Carlo moves specifically designed for long chain molecules. In this work, we have used Concerted Rotation (ConRot) [28], Double Bridging (DB) and Internal Double Rebridging (IDR) [29–32] moves. The DB move has been programmed for the strictly monodisperse case. Beside these three moves, reptation [33], configurational bias regrowth [34] and flip moves [35] have been used to sample the configurational space of the polymer chains. Translational and rotational moves were used for gas molecules as well as biased insertions and deletions to reach chemical equilibrium. Volume changes are applied to the system to maintain the imposed pressure (or equivalently the isotropic constraint σ_{iso}). Finally, the parallel "tempering" technique [36] has been used with 4 osmotic replica running independently, each one using regular osmotic ensemble moves. All replica are run at identical intensive and extensive variables, but the isotropic constraint. For randomly chosen pairs, an exchange between replica configurations having different isotropic constraint values is attempted. The reader is referred to the work by Banaszak et al. [26] for more details about the implementation of this move.

2.3. Force field description

The polymer studied in this work is a model of a linear polyethylene (PE) with 70 carbon atoms per chain. Selected gases are carbon dioxide, nitrogen and methane. Dispersion and repulsion interactions are described using a Lennard–Jones potential:

$$\begin{aligned} U(r) &= 4\varepsilon_{LJ}\left[\left(\frac{\sigma_{LJ}}{r}\right)^{12} - \left(\frac{\sigma_{LJ}}{r}\right)^{6}\right] \quad \text{for } r < r_c, \\ &= 0 \quad \text{else}, \end{aligned} \quad (3)$$

where r_c is the cutoff radius, r is the interparticle distance and ε_{LJ} and σ_{LJ} are the Lennard–Jones parameters. The cutoff radius value was fixed to 12 Å and standard tail corrections were applied [37]. Lennard–Jones parameters for all unlike interactions were obtained using Kong's combining rules [38] which have shown to give good predictions of fluid phase equilibria for several systems [39–42]. For carbon dioxide, the quadrupolar moment was described using partial charges. Coulombic potential energy, $U(r) = q_iq_j/4\pi\varepsilon_0 r$ was considered between these charges, where q_i is the value of the partial charge on atom i and ε_0 is the vacuum permittivity. Electrostatic interactions were computed using a standard implementation of the Ewald summation method [37]. A real space cutoff for electrostatic interactions of half the box size was used and other parameters were chosen such that the relative error in the reciprocal and real space be of the order of 10^{-5}.

The EPM2 model from Harris and Young [43] is used for CO_2. The molecule is treated as a rigid linear body, with C–O distance equal to 1.149 Å. Three Lennard–Jones sites and three partial charges located on each atom are used to represent dispersion–repulsion and electrostatic interactions. Nitrogen is modelled as a rigid dumbbell [21] with two Lennard–Jones centres separated by a distance of 1.0897 Å. Methane is described as a single Lennard–Jones site [44]. The anisotropic united atoms model AUA4 [45] has been used to describe dispersion–repulsion interactions for CH_2 and CH_3 groups in polyethylene. This potential has been shown to adequately describe liquid–vapor equilibria of pure hydrocarbons [46] and of hydrocarbons with different gases [45,47]. In the AUA4 model, CH_2 and CH_3 groups are represented by a Lennard–Jones particle and the hydrogen atoms are implicitly taken into account by shifting the centre of force from the carbon atom towards hydrogen atoms by a distance δ_{aua}. The non-bonded interaction parameters are listed in Table 1. Polyethylene chain flexibility is reproduced using bending and torsional [48] contributions. Carbon–carbon bond lengths are kept constant at 1.535 Å. Analytical expressions and parameters for intramolecular potentials for polyethylene are given in Table 2. Finally, intramolecular dispersion–repulsion interactions were considered between sites separated by at least four bonds.

3. Selected experimental data

In our approach, the *ad-hoc* constraint σ exerted on the amorphous phase is obtained so as to reproduce the solubility of experimentally well referenced semicrystalline systems. Because we expect that the constraint value is dependent upon crystallinity, we selected in the available literature experimental data obtained in the same range of temperature and crystallinity. The gathered data set is briefly presented below. From these data, the average solubility for each gas has been computed and used to obtain the constraint value and validate our methodology.

In order to quantify precisely the amount of absorbed gas in a polymer matrix, several experimental setups have been proposed in the literature, relying on two classes of methods. i) The dynamical approach where a pressure gradient is applied across the sample and the quantity of penetrant passing through the sample per time and area unit is monitored. Using the *time lag* method [49], solubility and diffusion coefficients are then obtained. ii) The static approach where the amount of dissolved gas is determined using either gravimetric or volumetric measurements.

Michaels and Bixler [11] measured the solubility of several simple gases (including CO_2, CH_4 and N_2) in semicrystalline polyethylenes with the two methods mentioned above. Data exist at 298 K, 0.1 MPa and crystalline volume fraction in the range 0.41–0.78. Both methods give results in good agreement. Ash et al. [50] also compared both methods and obtained a good agreement for CO_2 and N_2 solubility in a 45% crystallinity sample of

Table 1
Non-bonded interaction parameters used in this work.

	ε_{LJ}/k_B (K)	σ_{LJ} (Å)	δ_{AUA} (Å)	q (e)
PE				
CH_2	86.29	3.461	0.38	–
CH_3	120.15	3.607	0.22	–
CO_2				
C	28.129	2.757	–	+0.652
O	80.507	3.033	–	−0.326
N_2				
N	36.0	3.31	–	–
CH_4	149.92	3.733	–	–

Table 2
Bending and torsion potential functions and parameters used in this work for polyethylene. CH_x stands for methyl or methylene group. Energetic parameters K_θ and a_i are expressed in Kelvin.

Bending $V(\theta)/k_B = \frac{K_\theta}{2}(\cos\theta - \cos\theta_0)^2$	CH_x–CH_x–CH_x $\theta_0 = 114°$ $K_\theta = 74900$
Torsion $V(\phi)/k_B = \sum_{i=0}^{8} a_i \cos^i(\phi)$	CH_x–CH_x–CH_x–CH_x $a_0/\ldots/a_8 = 1001.36/2129.52/$ $-303.06/-3612.27/2226.71$ $11965.93/-4489.34/-1736.22/2817.37$

polyethylene. Flaconnèche et al. [51] used both static and dynamical approaches in the study of CO_2 permeability in polyethylene sample with 51% crystallinity. Naito et al. [52] using a dynamical approach with a 43% crystallinity sample, also obtained solubilities in very good agreement with Michaels data for several gases including CO_2, CH_4 and N_2. Solubility data in the amorphous phase (*i.e.* corrected from the crystalline amount) are gathered in Table 3.

Using a static approach, von Solms et al. [53] have recently measured solubilities under high pressure using a microbalance. The absorption cell is immersed in glycerine to maintain the temperature. Solubilities for CH_4 and CO_2 up to pressures of 16 MPa in polyethylene sample with a crystalline fraction of 63% are reported.

Using the same method, Li and Long [54] obtained solubilities in samples of 0.55 crystallinity at 298 K in the pressure range 2–8 MPa. As can be seen in Table 3, Li and Long values are quite different from those obtained by other authors.

In order to reduce the loss of gas between the absorption and desorption periods involved in the static approach, some enhancements have been proposed. Togawa et al. [55] introduced the freeze-purged-desorption technique, characterised by three periods of time based on the stepwise change in the system temperature. Using this method, they observed solubility notably higher than those observed by other authors. According to Togawa, this is related to the fact that their method avoids any gas loss during the transfers. Their measurements in a semicrystalline polyethylene with a crystalline fraction of 0.53 are reported in Table 3.

As can be seen from Table 3, there is an overall good agreement between gas solubilities obtained from these authors, with different methods and apparatus with the exception of Li and Long values. Consequently, we excluded this set of data from the computation of average solubilities for CH_4 and N_2. In order to account for the discrepancies between different author results, we computed the standard deviation of the mean. In the following, this last value will be used as an estimate of the error on the experimental data.

Table 3
Solubility constant of gases in amorphous phase of semicrystalline polyethylene, in g/100 g/MPa, evaluated from available experimental data as given in cited papers. All solubilities have been corrected from the crystalline fraction of the samples (see equation (1)). $<S_a>$ is the average of all the data except for CH_4 and N_2 where Li et al. values have been discarded. δS_a is the standard deviation. These solubility data have been measured at 298 K except that of Flaconnèche which have been obtained at 293 K.

Gas	CO_2	CH_4	N_2
Li [54]	–	0.233	0.260
Michaels [11]	0.932	0.153	0.054
Naito [52]	0.966	0.143	0.052
Ash [50]	1.180	–	0.061
Togawa [55]	1.379	–	–
von Solms [53,56]	0.772	0.096	–
Flaconnèche [51]	0.911	–	–
$<S_a>$	1.023	0.131	0.056
δS_a	0.081	0.014	0.002

4. Simulation results and discussion

We present on Fig. 1 CO_2 and CH_4 concentrations in amorphous polyethylene at 293 K and 298 K respectively, obtained from simulations in the osmotic ensemble. During these simulations, the isotropic constraint σ_{iso} is equal to the gas pressure, meaning that no additional constraint σ is imposed to the polymer rich phase. The values are compared with experimental data from Flaconnèche (CO_2) and Michaels (CH_4). Although a good agreement was observed at high temperature on the same systems modelled with the same methodology [42], the situation is less favourable at low temperature. Predictions clearly overestimate the absorbed quantities, roughly by a factor 4–5. As mentioned in the introduction, this behaviour was already observed in molecular simulations of amorphous polymer phases [21,22]: even with a correct force field, simulations at low temperature do not reproduce experimental solubilities.

We present on Fig. 2 the results of simulations in the osmotic ensemble for CO_2 in amorphous polyethylene at 293 K *versus* the additional constraint σ. Three different gas pressures have been investigated in the range 0.8–5 MPa. As expected, increasing σ decreases the gas concentration inside the simulated system. By applying an increasing constraint value, gas molecules are expelled from the polymer rich phase until the experimental concentration is recovered at some constraint value. Although this general behaviour is quite obvious, the interesting result is that the constraint value is independent of the gas pressure. Moreover, the same behaviour is observed with methane and nitrogen, as can be seen on Figs. 3 and 4. Therefore, a unique constraint value emerges, independent of the gas nature and pressure (at least in the pressure range investigated), with a value in the range 70–90 MPa. This result validates the assumption that was initially made: an *ad-hoc* constraint may reproduce an intrinsic property of the semicrystalline material.

An interesting feature of the osmotic ensemble (over the Grand Canonical ensemble for example) is its ability to give the swelling degree of the polymer phase, Q_a defined as:

$$Q_a = \frac{V^a_{\text{swell}} - V^a_{\text{bulk}}}{V^a_{\text{bulk}}}. \tag{4}$$

where V^a_{bulk} is the volume of the amorphous phase of the pure polymer and V^a_{swell} is the volume of the amorphous swollen phase.

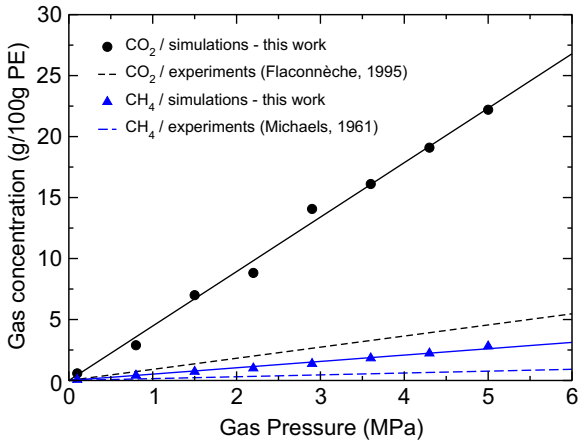

Fig. 1. CO_2 and CH_4 concentration in amorphous polyethylene at 293 K and 298 K respectively, *versus* gas pressure in the osmotic ensemble. The total isotropic constraint σ_{iso} is equal to the gas pressure, or equivalently, the additional constraint σ is equal to zero. Data are compared with experimental results of Michaels [11] for CH_4 and of Flaconnèche [51] for CO_2.

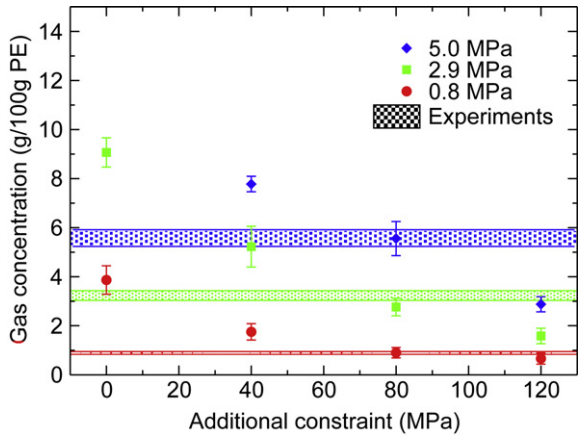

Fig. 2. CO_2 concentration in amorphous polyethylene at 293 K *versus* the additional constraint σ. Three different gas pressures have been investigated, in the range 0.8–5 MPa. Shaded areas correspond to average experimental values and standard deviation of the mean. The computed value at zero additional constraint for a gas pressure of 5 MPa is equal to 22.2 g/100 g PE. It is not reported here for clarity purposes.

V^a_{swell} is directly obtained from simulations in the osmotic ensemble, whereas V^a_{bulk} can be obtained from simple *NPT* simulations of the pure polymer. If one considers that the crystalline phase is not permeable to gases, the amorphous phase alone contributes to the total swelling Q of the semicrystalline material. We can simply write $Q = \phi_a Q_a$ where ϕ_a is the volume fraction of the amorphous phase in the pure semicrystalline material.

The swelling degree of the studied systems is given in Table 4, at the highest gas pressure investigated. Three different quantities are given: Q_a computed without additional constraint ($\sigma = 0$) and under the constraint which reproduces experimental solubilities ($\sigma = 80$ MPa), and Q. This last quantity was obtained from an amorphous phase content $\phi_a = 0.5$ and with the Q_a value obtained at $\sigma = 80$ MPa. As evidenced by the concentration values obtained for $\sigma = 0$, a large amount of gas is dissolved under such conditions, leading to a very high swelling for these systems. When the additional constraint is applied, much smaller swelling degrees are observed. We didn't find experimental swelling degree data for the systems studied. Boyer et al. [57] measured the solubility of CO_2 in semicrystalline polyethylene ($\phi_a = 0.55$) and fitted their data using the Sanchez–Lacombe equation of state (SL-EOS) by adjusting the

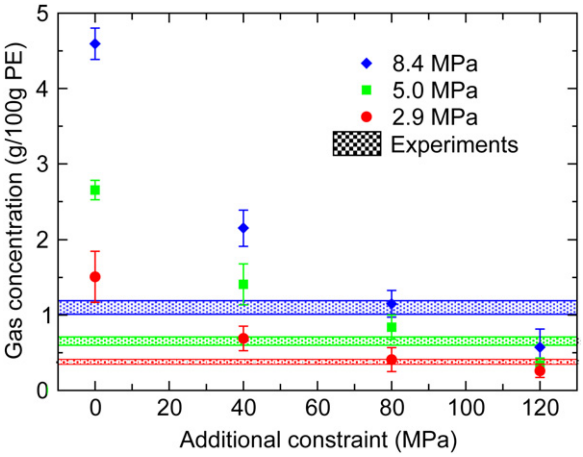

Fig. 3. CH_4 concentration in amorphous polyethylene at 298 K *versus* the additional constraint σ. Three different gas pressures have been investigated, in the range 2.9–8.4 MPa. Shaded areas correspond to average experimental values and standard deviation of the mean.

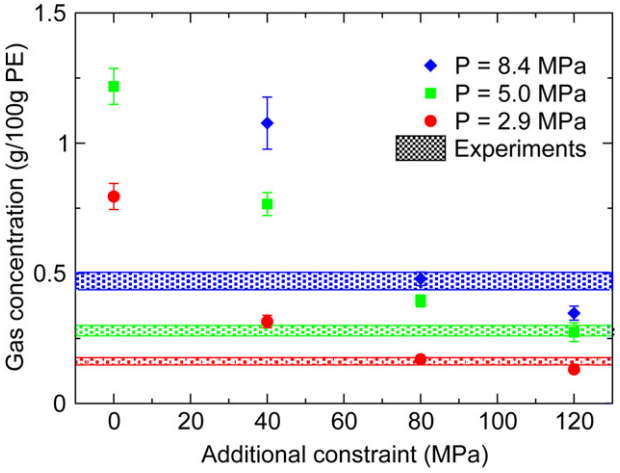

Fig. 4. N_2 concentration in amorphous polyethylene at 298 K *versus* the additional constraint σ. Three different gas pressures have been investigated, in the range 2.9–8.4 MPa. Shaded areas correspond to average experimental values and standard deviation of the mean.

binary interaction parameter k_{12} between CO_2 and polyethylene. The SL-EOS was then used to predict the swelling degree upon absorption. Q has been estimated to 2.1 percent at 333 K and 5 MPa, in good agreement with the value computed in this work.

The small swelling degree observed for the three gases studied here, reveals that solubilities in this pressure range could be obtained from constant volume simulations, e.g. from Grand Canonical ensemble Monte Carlo simulations (GCMC). It is important to notice here that the density of the pure polymer phase is a crucial input of the simulation. If the density of the pure amorphous polymer phase calculated without additional constraint is used, solubilities will be overestimated for semicrystalline materials. If the density of the pure polymer phase obtained under the additional constraint σ is used, computed solubilities are in good agreement with those obtained in the osmotic ensemble (see Supplementary informations for details). Nevertheless, simulations in the osmotic ensemble are the most appropriate, especially if significant swelling is expected.

The additional constraint σ deduced from our simulations is *a priori* supposed to account for both elastic and local density effects. The elastic effect contribution must be related to the swelling degree. Because the additional constraint value is independent of the swelling degree, we can conclude that σ, at least in the pressure range investigated here, accounts mostly for the local density effect: the applied stress acts on the effective density of the permeable phase. This effective density is found to be 873 ± 3 kg/m^3 at 298 K under the additional constraint which corresponds to an increase of 3% compared to the non constrained value. The mean end-to-end square distance is not significantly affected by the use of this extra constraint ($< R^2_{ee} > = 1275 \pm 9$ A^2 at $\sigma = 0$, $< R^2_{ee} > = 1289 \pm 8$ A^2 at $\sigma = 80$ MPa). This is consistent with the small density change introduced here.

Table 4
Swelling degree of polyethylene with N_2, CH_4 and CO_2 at given pressure and temperature. Q_a is the amorphous phase swelling computed directly from Monte Carlo simulations. Q is a prediction of the semicrystalline material swelling given an amorphous volume fraction of ≈0.5.

	N_2	CH_4	CO_2
P (MPa)	8.4	8.4	5
T (K)	298	298	293
Q_a, $\sigma = 0$	5% ± 2.8	11.2% ± 2.6	20% ± 1.6
Q_a, $\sigma = 80$ MPa	1% ± 1	2.4% ± 1.4	3% ± 0.8
Q, $\sigma = 80$ MPa	0.5% ± 0.5	1.2% ± 0.7	1.5% ± 0.4

A variety of experimental methods have shown that a significant interfacial region exists in semicrystalline polymers, between crystalline and disordered regions. Mandelkern et al. [19], using Raman internal and longitudinal acoustical modes, measured the thickness of the interfacial region in linear polyethylene. The thickness is found to depend on the polymer molecular weight. For a molecular mass of the order of 10^5 g/mol, the interfacial region thickness is ~25 Å while the crystallite and the disordered regions have respectively thicknesses of 150 Å and 110 Å. These results are in good agreement with small-angle-X-ray scattering (SAXS) experiments [58]. Using ^{13}C NMR, Kitamaru et al. [59] were able to distinguish between three different regions and found an interfacial thickness of the order of 15–20 Å. From theoretical expressions based on a lattice model, Kumar and Yoon [60] concluded that the interfacial thickness should range between 10 and 30 Å in most cases. In a more recent work, Hedesiu et al. [61] have investigated the effect of temperature on phase composition (crystalline, amorphous and interfacial regions), molecular mobility and thickness of domains in high density polyethylene using different experimental techniques. The domain thickness determined by NMR is in good agreement with those measured by SAXS and transmission electron microscopy (TEM) on the same sample. It is shown there that the fraction of crystalline regions decreases with increasing temperature in the range 40–110 °C, while content of interfacial and amorphous phases increases.

Therefore, as the morphology of semicrystalline polymers evolves with temperature, we expect that the effective density (hence σ) of the permeable phase changes with temperature (or with the crystalline fraction of the material). In order to evaluate the influence of the temperature on σ, we have computed solubility of N_2, CH_4 and CO_2 in polyethylene at 333 K. We used osmotic ensemble simulations, at a single gas pressure of 5 MPa, for several σ_{iso} values. The additional constraint value was determined using experimental data from Ash [50] and Serpe [62] and the same methodology as described above. It is important to notice here that less data are available at this temperature, which makes the determination of σ more uncertain. However, the general tendency is a net decrease of the constraint value, from 80 ± 10 MPa at low temperature (293 and 298 K depending on the gas) to roughly 60 ± 10 MPa at 333 K. The corresponding curves calculated at a gas pressure of 5 MPa for the three studied species are given in Supplementary informations. This behaviour supports our interpretation of the meaning of the additional constraint σ: with an increase in temperature, the crystalline fraction decreases along with the effective density (hence σ).

A final comment must be done about the magnitude of the additional constraint σ. Because the role of σ is to bring the simulated amorphous phase to an effective density of the real permeable phase, every factor which affects the density of the polymer model will affect the value of σ. Therefore, the values obtained here for σ are meaningful only in the case of the particular force field used here.

5. Conclusion

We have employed Monte Carlo simulations to study the solubility of simple gases in semicrystalline polyethylene. Our motivation was to investigate the influence of the complex morphology of semicrystalline polymers onto gas solubility. Based on experimental evidences [63,59,20,64,61], it is known that semicrystalline polymers exhibit crystalline, amorphous and interfacial regions, the permeable region being formed by both the amorphous and the interfacial regions.

Our simulations confirm, in agreement with previous works, that the solubility computed in the pure amorphous phase is significantly larger than experimental measurements. From simulation results in the melt state for the same systems, which have proven to be in good agreement with experiments [42], we can conclude that these differences cannot be attributed to the force field or the Monte Carlo sampling used. Clearly, the problem comes from the description of the permeable phase in the semicrystalline state.

By using the osmotic ensemble in an original way, we have been able to show that experimental solubilities are reproduced when a *single* additional constraint value, σ, is applied to the polymer phase. The important point is that the applied constraint does not depend on the gas pressure (in the range 0–8 MPa) or nature (for N_2, CH_4 and CO_2). Rather, it is a characteristic of the polymer at a given temperature and crystallinity degree. We have seen that this constraint has to be applied even with weakly soluble gases (like N_2) at low pressure, where almost no swelling is observed. We can therefore conclude that the role of the *ad-hoc* constraint is to reproduce the effective density of the real material.

The predictive capability of molecular simulations for the calculation of solubility in semicrystalline state is therefore limited by the knowledge of this effective density. The methodology employed here, based on the evaluation of this quantity from some experimental data and coupled with Monte Carlo simulations in the osmotic ensemble is a possible route, although a precise description at a molecular level of the structure of the interfacial region would be the method of choice.

Acknowledgments

Bruno Flaconnèche and Marie-Hélène Klopffer (IFP Energies nouvelles) are gratefully acknowledged for providing us with experimental data. Jean-Marie Teuler (Laboratoire de Chimie Physique) is gratefully acknowledged for support in code development. One of us (PM) would like to thank IFP Energies nouvelles and the Agence Nationale de la Recherche et de la Technologie (ANRT) for financial support through a PhD grant. The authors would like to acknowledge the support of the French *Agence Nationale de la Recherche* (ANR) under grant SUSHI (grant No. 07-BLAN-0268) "SimUlation de Systèmes Hétérogènes et d'Interfaces".

Appendix. Supplementary data

Supplementary data associated with this article can be found in the on-line version, at doi:10.1016/j.polymer.2010.08.020.

References

[1] Gusev AA, Suter UW. Theory for solubility in static systems. Phys Rev A 1991;43(12):6488–94.
[2] Müller-Plathe F. Calculation of the free energy for gas absorption in amorphous polypropylene. Macromolecules 1991;24:6475–9.
[3] Widom BJ. Some topics in the theory of fluids. J Chem Phys 1963;39:2808–12.
[4] de Pablo JJ, Laso M, Suter UW. Simulation of the solubility of alkanes in polyethylene. Macromolecules 1993;26:6180–3.
[5] Pant PVK, Boyd RH. Molecular dynamics simulation of diffusion of small penetrants in polymers. Macromolecules 1993;26(4):679–86.
[6] Cuthbert TR, Wagner NJ, Paulaitis ME, Murgia G, D'Aguanno B. Molecular dynamics simulation of penetrant diffusion in amorphous polypropylene: diffusion mechanisms and simulation size effects. Macromolecules 1999;32:5017–28.
[7] Eslami H, Muller-Plathe F. Molecular dynamics simulation of sorption of gases in polystyrene. Macromolecules 2007;40(17):6413–21.
[8] Kucukpinar E, Doruker P. Molecular simulations of small gas diffusion and solubility in copolymers of styrene. Polymer 2003;44:3607–20.
[9] Neyertz S, Brown D. Influence of system size in molecular dynamics simulations of gas permeation in glassy polymers. Macromolecules 2004;37(26):10109–22.
[10] Cozmuta I, Blanco M, Goddard WA III. Gas sorption and barrier properties of polymeric membranes from molecular dynamics and Monte Carlo simulations. J Phys Chem B 2007;111:3151–66.
[11] Michaels AS, Bixler HJ. Sorption of gases in polyethylene. J Polym Sci 1961;50:393–412.

[12] Compan V, Castillo LFD, Hernandez SI, Lopez-Gonzalez MM, Riande E. On the crystallinity effect on the gas sorption in semicrystalline linear low density polyethylene (LLDPE). J Polym Sci Part B Polym Phys 2007;45(14):1798–807.
[13] Rogers CE, Stannett V, Szwarc M. The sorption of organic vapors by polyethylene. J Phys Chem 1959;63(9):1406–13.
[14] Michaels AS, Hausslein RW. Elastic factors controlling sorption and transport properties of polyethylene. J Polym Sci Part C 1965;10:61–2.
[15] Doong SJ, Ho WSW. Sorption of organic vapors in polyethylene. Ind Eng Chem Res 1991;30(6):1351–61.
[16] Banaszak BJ, Lo D, Widya T, Ray WH, de Pablo JJ, Novak A, et al. Ethylene and 1-hexene sorption in LLDPE under typical gas-phase reactor conditions: a priori simulation and modeling for prediction of experimental observations. Macromolecules 2004;37:9139–50.
[17] Serna LV, Becker JL, Galdamez JR, Danner RP, Duda JL. Elastic effects on solubility in semicrystalline polymers. J Appl Polym Sci 2008;107(1):138–46.
[18] Flory PJ. Thermodynamics of crystallization in high polymers. IV. A theory of crystalline states and fusion in polymers, copolymers and their mixtures with diluents. J Chem Phys 1949;17(3):223–40.
[19] Mandelkern L. The structure of crystalline polymers. Acc Chem Res 1990;23 (11):380–6.
[20] Hedenqvist M, Gedde UW. Diffusion of small-molecule penetrants in semicrystalline polymers. Prog Polym Sci 1996;21(2):299–333.
[21] Nath SK, de Pablo JJ. Solubility of small molecules and their mixtures in polyethylene. J Phys Chem B 1999;103:3539–44.
[22] Hu N, Fried J. The atomistic simulation of the gas permeability of poly(organophosphazenes). Part 2. Poly-[bis(2,2,2-trifluoroethoxy)phosphazene]. Polymer 2005;46(12):4330–43.
[23] Mehta M, Kofke DA. Coexistence diagrams of mixtures by molecular simulation. Chem Eng Sci 1994;49(16):2633–45.
[24] Spyriouni T, Economou IG, Theodorou DN. Phase equilibria of mixtures containing chain molecules predicted through a novel simulation scheme. Phys Rev Lett 1998;80(20):4466–9.
[25] Escobedo FA. Novel pseudoensembles for simulation of multicomponent phase equilibria. J Chem Phys 1998;108(21):8761–72.
[26] Banaszak BJ, Faller R, de Pablo JJ. Simulation of the effects of chain architecture on the sorption of ethylene in polyethylene. J Chem Phys 2004;120 (23):11304–15.
[27] Panagiotopoulos AZ, Stapleton MR. The Gibbs method for molecular-based computer-simulations of phase-equilibria. Fluid Phase Equilibria 1989;53:133–41.
[28] Dodd LR, Boone TD, Theodorou DN. A concerted rotation algorithm for atomistic Monte-Carlo simulation of polymer melts and glasses. Mol Phys 1993;78(4):961–96.
[29] Mavrantzas VG, Boone TD, Zervopoulou EZ, Theodorou DN. End-bridging Monte Carlo: a fast algorithm for atomistic simulation of condensed phases of long polymer chains. Macromolecules 1999;32(15):5072–96.
[30] Karayiannis NC, Mavrantzas VG, Theodorou DN. A novel Monte Carlo scheme for rapid equilibration of atomistic model polymer systems of precisely defined molecular architecture. Phys Rev Lett 2002;88(10):105503.
[31] Karayiannis NC, Giannousaki AE, Mavrantzas VG, Theodorou DN. Atomistic Monte Carlo simulation of strictly monodisperse long polyethylene melts through a generalized chain bridging algorithm. J Chem Phys 2002;117 (11):5465–79.
[32] Theodorou DN. Understanding and predicting structure–property relations in polymeric materials through molecular simulations. Mol Phys 2004;102 (2):147–66.
[33] Boyd RH. An off-lattice constant-pressure simulation of liquid polymethylene. Macromolecules 1989;22(5):2477–81.
[34] de Pablo JJ, Laso M, Suter UW. Simulation of polyethylene above and below the melting point simulation of polyethylene above and below the melting point. J Chem Phys 1992;96(3):2395–403.
[35] Bourasseau E, Ungerer P, Boutin A, Fuchs AH. Monte Carlo simulation of branched alkanes and long chain n-alkanes with anisotropic united atoms intermolecular potential. Mol Sim 2002;28(4):317–36.
[36] Swendsen RH, Wang JS. Replica Monte Carlo simulation of spin glasses. Phys Rev Lett 1986;57:2607–9.
[37] Allen MP, Tildesley DJ. Computer simulation of liquids. Oxford: Oxford Science Publications; 1989.
[38] Kong CY. Combining rules for intermolecular potential parameters. II. Rules for the Lennard-Jones (12-6) potential and the Morse potential. J Chem Phys 1973;59(5):2464–7.
[39] Potoff J, Errington J, Panagiotopoulos A. Molecular simulation of phase equilibria for mixtures of polar and non-polar components. Mol Phys 1999;97 (10):1073–83.
[40] Delhommelle J, Evans DJ. Configurational temperature profile in confined fluids. I. atomic fluid. J Chem Phys 2001;114(14):6229–35.
[41] Ungerer P, Wender A, Demoulin G, Bourasseau E, Mougin P. Application of gibbs ensemble and npt monte carlo simulation to the development of improved processes for H_2S-rich gases. Mol Simulation 2004;30:631–48.
[42] Faure F, Rousseau B, Lachet V, Ungerer P. Molecular simulation of the solubility and diffusion of carbon dioxide and hydrogensulfide in polyethylene melts. Fluid Phase Equilibria 2007;261(1–2):168–75.
[43] Harris JG, Yung KH. Carbon dioxide's liquid–vapor coexistence curve and critical properties as predicted by a simple molecular model. J Phys Chem 1995;99:12021–4.
[44] Möller D, Óprzynski J, Müller A, Fischer J. Prediction of thermodynamic properties of fluid mixtures by molecular dynamics simulations: methane–ethane. Mol Phys 1992;75(2):363–78.
[45] Ungerer P, Beauvais C, Delhommelle J, Boutin A, Rousseau B, Fuchs AH. Optimization of the anisotropic united atoms intermolecular potential for n-alkanes. J Chem Phys 2000;112(12):5499–510.
[46] Ungerer P, Nieto-Draghi C, Rousseau B, Ahunbay G, Lachet V. Molecular simulation of the thermophysical properties of fluids: from understanding toward quantitative predictions. J Mol Liq 2007;134(1–3):71–89.
[47] Ungerer P, Nieto-Draghi C, Lachet V, Wender A, di Lella A, Boutin A, et al. Molecular simulation applied to fluid properties in the oil and gas industry. Mol Simulation 2007;33(4–5):287–304.
[48] Toxvaerd S. Equation of state of alkanes II. J Chem Phys 1997;107 (13):5197–204.
[49] Klopffer M-H, Flaconnèche B, Odru P. Transport properties of gas mixtures through polyethylene. Plas Rubber Compos 2007;36(5):184–9.
[50] Ash R, Barrer RM, Palmer DG. Solubility and transport of gases in nylon and polyethylene. Polymer 1970;11:421–35.
[51] Flaconnèche B. Private communication.
[52] Naito Y, Mizoguchi K, Terada K, Kamia Y. The effect of pressure on gas permeation through semicrystalline polymers above the glass transition temperature. J Polym Sci Polym Phys 1991;29:457–62.
[53] von Solms N, Nielsen JK, Hassager O, Rubin A, Dandekar AY, Andersen SI, et al. Direct measurement of gas solubilities in polymers with a high-pressure microbalance. J Appl Polym Sci 2004;91(3):1476–88.
[54] Li NN, Long RB. Permeation through plastic films. AIChE J 1969;15:73–80.
[55] Togawa J, Horiuchi J-I, Kanno T, Kobayashi M. Freeze-purged-desorption method for quantitative evaluation of CO_2-solubility in polymeric films. J Memb Sci 2001;182:125–8.
[56] von Solms N, Michelsen ML, Kontogeorgis GM. Prediction and correlation of high-pressure gas solubility in polymers with simplified PC-saft. Ind Eng Chem Res 2005;44(9):3330–5.
[57] Boyer SAE, Grolier JPE. Simultaneous measurement of the concentration of a supercritical gas absorbed in a polymer and of the concomitant change in volume of the polymer. the coupled VW-pVT technique revisited. Polymer 2005;46(11):3737–47.
[58] Robelin-Souffaché E, Rault J. Origin of the long period and crystallinity in quenched semicrystalline polymers. 1. Macromolecules 1989;22(9):3581–94.
[59] Kitamaru R, Horii F, Murayama K. Phase structure of lamellar crystalline polyethylene by solid-state high-resolution 13C NMR: detection of the crystalline–amorphous interphase. Macromolecules 1986;19(3):636–43.
[60] Kumar SK, Yoon DY. Lattice model for crystal amorphous interphases in lamellar semicrystalline polymers – Effects of tight-fold energy and chain incidence density. Macromolecules 1989;22(8):3458–65.
[61] Hedesiu C, Demco DE, Kleppinger R, Buda AA, Bluemich B, Remerie K, et al. The effect of temperature and annealing on the phase composition, molecular mobility and the thickness of domains in high-density polyethylene. Polymer 2007;48(3):763–77.
[62] Serpe G. Perméabilité des polyéthylènes aux gaz sous moyenne pression et en température. Tech Rep IFP; 1995.
[63] Mandelkern L, Alamo RG, Kennedy MA. Interphase thickness of linear polyethylene. Macromolecules 1990;23(21):4721–3.
[64] Wang M, Bernard GM, Wasylishen RE, Choi P. A solid-state C-13 NMR investigation of the morphology of single-site and Ziegler–Natta linear low-density polyethylenes with varying branch contents. Macromolecules 2007;40(18):6594–9.